Springer

Journal of Mechanical Science and Technology 23 (2009) 89~99

Journal of Mechanical Science and Technology

www.springerlink.com/content/1738-494x
DOI 10.1007/s12206-008-0925-4

Load effect on the vibration characteristics of a stage with rolling guides †

Jui Pin Hung*

Department of Mechanical Engineering, National Chin-Yi University of Technology, Taiping, Taiwan

(Manuscript Received April 8, 2008; Revised September 5, 2008; Accepted September 23, 2008)

Abstract

This paper aims to investigate the dynamic characteristics of a loading stage with a rolling guide. In practice, the rolling guide is designed with different contact geometries to withstand various loads in service; it forms a rolling interface with contact stiffness varying with the applied loads. To model the rolling contact mode realistically, different contact modes were assumed at the interfaces between the ball and raceway and simulated by using spring elements with stiffness calculated by using the Hertzian contact theorem. The vibration characteristics of the rolling guide were determined by the proposed method and successfully verified by experimental vibration tests. As validation of the proposed method, a loading stage with rolling guides was also demonstrated to have different dynamic characteristics as various loads were applied, with the results from the experiments correlating to the finite element simulations.

Keywords: Contact stiffness; Hertz theory; Modal analysis; Rolling guide

1. Introduction

In recent years, the linear rolling guide (Fig. 1) has been widely used for high-precision positioning systems in applications such as CNC machine tools, semiconductor manufacturing equipment, and inspection apparatus because of its superiority over conventional sliding linear motion bearings. In such positioning systems, rolling interfaces exist between the rolling balls and the raceways. As in the case of ball bearings, the rolling contact for the linear guide is regarded as Hertzian contact status, where the contact stiffness at the interface between the ball and ball groove significantly affects the dynamic behavior of the linear bearings [1-5]. Additionally, in practical applications of linear guides an oversized rolling ball is used to produce the preload effect, which increases the structural rigidity and load-carrying ability of the linear guide. According to previous studies [3-5], a preloaded linear guide will have different vibration characteristics due to the change in contact stiffness at the ball grooves, which has been verified to vary with the magnitude of the preload setting on the rolling balls. This directly affects the stiffness and dynamic behavior of the overall structure of the linear guide mechanism. Therefore, understanding the interface dynamics in the designing stage is a prerequisite to accurately predict the structural performance of a positioning mechanism with rolling guides.

Early investigations on the vibration characteristics of ball bearings were conducted by Harries [6, 7] and Shin [8], and then followed up by applications of the linear guide by Kasai [9] and Ye et al. [10]. Kasai demonstrated that the rolling balls passing in a recirculating mechanism were the main cause for the vibration of a linear guide in motion. Ye et al. demonstrated the rigid-body free vibration of the carriage by conducting a modal analysis on the linear guide. Recently, Ohta et al. [2, 3] conducted a vibration analysis on the linear guide mechanism using analytical

† This paper was recommended for publication in revised form by Associate Editor Jeong Sam Han

* Corresponding author. Tel.: +886 4 23924505, Fax.: +886 4 23939932
E-mail address: hungjp@ncut.edu.tw

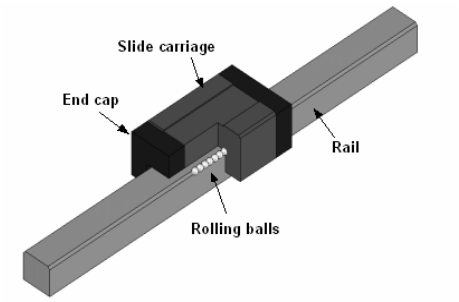

Fig. 1. Assembly of a linear guide of low profile.

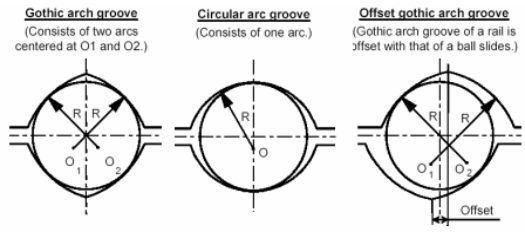

Fig. 2. Three types of contact geometry of ball groove of a rolling guide [12].

and finite element approaches. In their analytical approach, the linear guide was regarded as a rigid body and simulated by a spring-mass system with multiple degrees of freedom. In their finite element analysis, the rolling interface of the ball groove was modeled as a point-to-point contact mode with a spring element. Chang [4] and Wu [5] also employed the finite element approach to predict the vibration characteristics of rolling guides with different preloads. In their finite element models of the linear guide, the rolling interface was modeled as a surface contact mode by introducing a contact element of zero thickness at the rolling interface.

These studies show that modeling the rolling interface associated with contact stiffness is important for vibration analysis. It is also worth noting that the spring constant adopted in Ohta et al.'s model [2, 3] was taken from the vertical stiffness of the guide structure, whereas the contact stiffness used by Chang and Wu [4, 5] was calculated according to the Hertz theorem [11], which is believed to realistically reflect the contact status of the guide. However, to model the rolling ball while processing the finite element model is a troublesome task. Besides, a commercialized rolling guide is often designed with two or four rows of ball grooves with a circular or Gothic contact profile, which can cause more complicated contact conditions at the rolling interface. Using spring or surface contact elements in simulating the rolling interface should be an efficient way to create an analysis model with sufficient accuracy. Moreover, simulating the rolling interface at the ball groove to account for the effect of the rolling balls needs to be considered. Based upon this concept, this study proposes a simplified method for modeling the rolling interface of a linear guide designed with different contact geometries. This proposed new model employs finite element modal analysis and was verified by vibration modal tests of the preloaded linear guides. Further validation of the proposed method for applications was carried out on a loading stage with rolling guides.

2. Contact stiffness of the rolling interface

Generally, the contact geometry of a rolling guide can be classified into three types which can provide sufficient load-carrying capacity for different operating conditions in practical applications, shown in Fig. 2 [12]. The rolling guide used in this study was designed with four rows of rolling balls, as shown in Fig. 3 [13]. Each ball groove has a contact profile of a circular arc forming a two-point contact mode, rather than the four-point contact status which occurs in a Gothic groove. This contact mode is similar to the case for ball bearings and can be modeled according to the Hertz theory. Therefore, the contact force between the rolling ball and the raceway of the groove is related to the local deformation occurring at the contact point, expressed in Eq. (1) [11]:

$$Q = K_h \alpha^{3/2} \tag{1}$$

where Q is the contact force and α is the elastic deformation at the contact point. K_h represents the Hertz constant and can be determined from the following parameters [14, 15]:

$$k = 1.0339\left(\frac{C_y}{C_x}\right)^{0.6360} \tag{2}$$

$$K_h = \frac{\pi k E'}{3f}\sqrt{\frac{2C\varepsilon}{f}} \tag{3}$$

$$f = 1.5277 + 0.6032\,ln\left(\frac{C_y}{C_x}\right) \tag{4}$$

$$\varepsilon = 1.0003 + 0.5968\left(\frac{C_x}{C_y}\right) \tag{5}$$

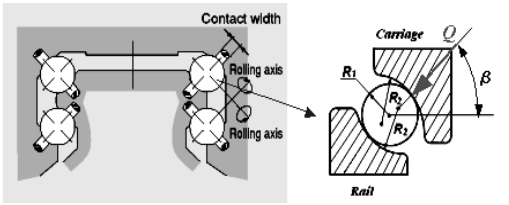

Fig. 3. Schematic of contact geometry of rolling guide with four rows of rolling balls, forming a two point contact mode within each ball groove. In the figure, *β and Q* represent the contact angle and contact force, R_1 and R_2 are the radii of rolling ball and ball groove, respectively.

$$E' = 2/(1-\mu_a^2)/E_a + (1-\mu_b^2)/E_b \tag{6}$$

E is Young's modulus, μ is Poisson's ratio of material and constants, and C, C_x, C_y are related to the diameter D of the rolling ball and the radius R_i of the raceway; these can be expressed as follows, in terms of the form factor f_i of the contact geometry of the raceway:

$$C_x = \frac{D}{2} \quad C_y = D\frac{f_i}{2f_i - 1} \quad C = \frac{C_x C_y}{C_y - C_x} \tag{7}$$

From Eq. (1), the normal stiffness K_n can then be expressed as

$$K_n = \frac{dQ}{d\delta} = \frac{3}{2}K_h\delta^{1/2} = \frac{3}{2}K_h^{2/3}Q^{1/3} \tag{8}$$

It is evident from the above equations that the contact stiffness in the normal direction is dependent upon the contact load. Hence, the preload on the rolling ball and the external loading imposed on the slider will affect the contact stiffness at the rolling interface. The dynamic characteristic that varies with the loads on the linear guide is therefore below expectations.

3. Vibration analysis of the rolling guide

3.1 Vibration test

This section discusses the vibration test carried out on the commercialized linear guide to realize the vibration characteristics. The typical vibration modes of a linear guide are characterized as pitching, rolling, yawing, and vertical motions, as shown in Fig. 4. Fig. 5 illustrates the experimental configuration. The linear guide was placed on a graphite bed and the accelerometer was mounted on the

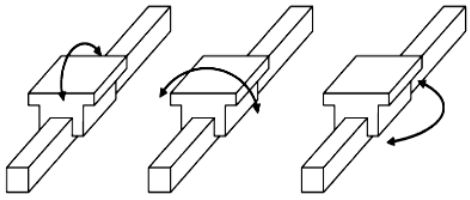

(a) Pitching motion (b) Rolling motion (c) Yawing motion

Fig. 4. Typical vibration motions of a linear guide.

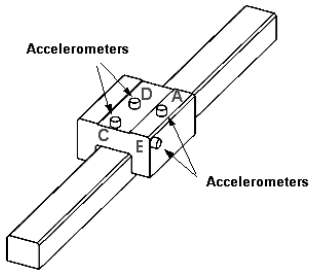

Fig. 5. Configuration of vibration test, showing the locations of accelerometers A, B, C and D for measuring the vibration motion of rolling, yawing, pitching, and vertical mode, respectively.

carriage to measure the vibration response in different directions. As shown in Fig. 5, the accelerometer was used at positions A, B, C, and D to measure the vibration motions of the rolling, yawing, pitching, and vertical modes, respectively. In essence, the measuring positions were the points where the vibration peak corresponding to the vibration motion in a certain direction occurred, which can be accurately predicted by finite element modal analysis. The accelerometer sensitivity was 100 mV/g, and an impulse hammer with a force sensor and white plastic tip was used to excite the guide at various levels.

In the experiments, the vibration spectrum was recorded by a digital analyzer that measures the natural frequency by hammering the slide carriage in the measured direction. In addition, the rolling guide with different preloads, a slight preload of 78.3 N and a heavy preload of 548.1 N, was tested to investigate the preload effect on the vibration frequency and for further verification of the finite element predictions. The geometric specifications for the linear guide are listed in Table 1.

3.2 Finite element modal analysis

Fig. 6(a) shows the finite element mode of the

Table 1. Geometry specification of a linear guide used in test and analysis.

Carriage length, width, height	39.8, 34, 19.5 mm
Rail width, height	15, 12.5 mm
Nominal diameter of steel ball	2.778 mm
Contact angle, β	45
Dynamic rated load, C	7830 N
Preload setting low preload high preload	 78.3 N (0.0l C) 548.1 N (0.07C)
Form factor, f	0.52
Total number of balls	60

rolling guide used in the vibration experiment, which consists of a rail, slide carriage, rolling balls, and end cape. The rail and carriage were made of nickel-chromium-molybdenum steel (elastic modulus E = 206 GPa, density ρ = 7800 kg/m^3), and the end cape was plastic (elastic modulus E = 3.57 GPa, density ρ = 1400 kg/m^3). A Poisson's ratio of 0.3 was used for all the three materials.

The rolling guide was meshed with brick elements and the resulting mode contained 9310 elements and 13206 nodes. Note that the rolling guide has four rows of rolling balls, which form a two-point contact state at each ball groove as the grooves have a circular profile. To avoid the complexity in mesh generation of the rolling grooves in the finite element model, the four rolling grooves were simplified to two (Fig. 6(b)), but with equivalent contact stiffness at the rolling interface as that of the original guide model.

Moreover, the rolling interfaces between the rolling balls and raceways were modeled as the two contact modes shown in Fig. 6c. The first mode is similar to those established in previous studies [2-5]. However, here the rolling balls were simulated with mass elements of equivalent ball weight, and the contact interfaces at ball grooves were modeled with two point-to-point spring elements (Fig. 6(c)), rather than the surface contact elements used by Chang[4]. In addition, the contact stiffness used in this mode was different from that used by Ohta et al. [2], which measures the vertical stiffness of the linear guide in the compression test. In the second mode, the carriage and guideway were directly connected by using spring elements by intentionally neglecting the rolling balls, but the overall spring

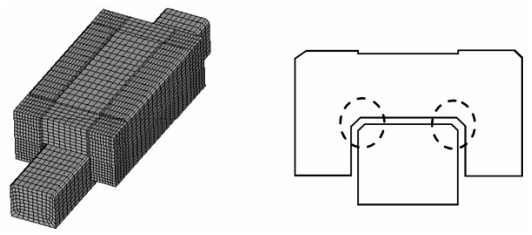

(a) Finite element model (b) Guide with two ball grooves

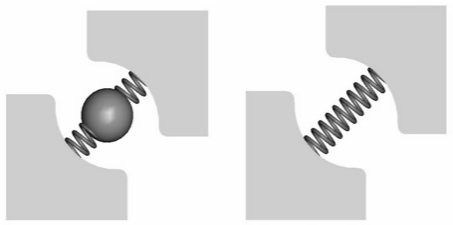

(c) Two different contact modes assumed at the rolling interface between ball and raceways

Fig. 6. Finite element model of a low profile linear guide, in which the rolling interface at the ball groove was modeled in two ways, (1) two spring elements at contact interface between ball and the raceways of rail and slide, respectively. (2) single spring element connecting rail and slide carriage.

elements had a stiffness that was the same as the first mode. This second mode was expected to greatly increase the efficiency in preparing the analysis model without loss of accuracy of the results.

As they all had the same contact geometry, all of the interfaces between the rolling balls and grooves had the same contact stiffness. Based upon the specifications of the rolling guide (Table 1), the stiffness at any contact point was calculated as K_n = 19.75 N/μm for the heavy preload and K_n = 10.325 N/μm for the slight preload. The vibration characteristics of the rolling guide were obtained by implementing the modal analysis into finite element computation.

3.3 Results and discussions

The fundamental vibration mode shapes developed from the results of the finite element modal analysis of the rolling guide with slight preload are graphically depicted in Fig. 7. As shown there, the carriage vibrates in different modes– rolling, pitching, yawing, and vertical motions, in accordance with the direction of the motion (Fig. 5). For a slightly preloaded guide simulated with different rolling contact mode, the predicted order of natural fre-

Table 2. Comparisons of the natural frequencies linear guide with different preload (unit: kHz).

Vibration mode	Low preload (K_n = 10.325 N/μ m)			High preload (K_n = 19.75 N/μ m)		
	Finite element prediction		Vibration test	Finite element prediction		Vibration test
	Without	With		Without	With	
Yawing	3.19 (0.6%)	3.17 (0.0%)	3.17	4.08 (1.7%)	4.01 (0.0%)	4.01
Pitching	4.10 (3.0%)	4.08 (2.5%)	3.98	5.50 (5.8%)	5.44 (4.6%)	5.20
Vertical	4.67 (7.9%)	4.64 (7.4%)	4.33	6.28 (2.1%)	6.21 (1.0%)	6.15
Rolling	6.16 (3.0%)	6.12 (2.3%)	5.98	8.19 (1.2%)	8.12 (0.4%)	8.09

Note: Values in parentheses represent the percentage differences between the finite element predictions and experimental measurements.

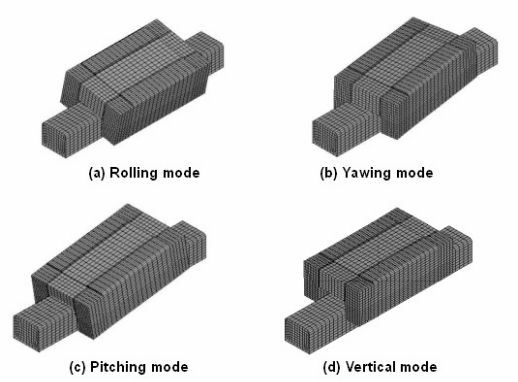

Fig. 7. Fundamental vibration mode shapes of a linear guide.

quencies is yawing (3.17~3.19 kHz), pitching (4.08~4.10 kHz), vertical motion (4.64~4.67 kHz), and rolling (6.12~6.16 kHz). The current analysis in the literature of this field predicts a similar trend in the sequence of vibration frequency [2-5]. In addition, Table 2 indicates that the natural frequency of the guide is affected by the preload setting on the rolling balls. Obviously, a linear guide with a heavy preload will induce higher contact stiffness upon the rolling interface than those with a low or slight preload, and hence will vibrate at a higher frequency.

The vibration spectra measured by different accelerometers are illustrated in Figs. 8 and 9 for a linear guide with a light and heavy preload, respectively, where the vertical axis represents the ratio of the vibration acceleration to the force triggered by the hammer. The main peaks of each spectrum can be identified as the natural frequency corresponding to the mode shape that was predicted by the finite element analysis. As observed in Figs. 8 and 9, the heavy preloaded guide shows a vibration spectrum similar to that of the guide with lower preload, but their vibration peaks are found to occur at different natural frequencies: a linear guide with a heavy preload possesses higher free vibration frequencies. Further comparison of the results in Table 2 reveals that the frequencies predicted by the finite element model agree with the experimental measurements: there is a maximum percentage difference of less than 8%, regardless of the preload (slight or heavy) of the rolling guide.

Moreover, the estimates of the linear guides with different contact modes assumed at the rolling interface were very accurate, with a maximum percentage difference of 0.08% with the results. This apparently demonstrates that the rolling balls had no significant effect on the vibration motions of the rolling guide. Therefore, modeling the contact interface using spring elements to directly connect the carriage and rail can accurately predict the vibration characteristics of the linear guide. This again presumes that the proposed analysis model associated with the modal tests is a feasible way to accurately predict the dynamic behavior of a loading stage with a rolling guide.

4. Vibration analysis of the stage

To verify the effectiveness of the proposed approach, a simplified loading stage was constructed for modal analysis to investigate the load effect on the stiffness of the guide as well as the vibration characteristics of the stage. As shown in Fig. 10, the platform is horizontally supported by the carriages of the linear guides mounted on the base. This allows the platform to move freely along the linear guide without an actuator. As stated in the previous section, a linear guide with different preloads will experience vibration motions at different frequencies. In addition, Eq. (8) shows that the contact stiffness at the rolling interface is closely related to the contact force acting on the rolling balls. The external loads imposed on the stage may further induce different reactions at

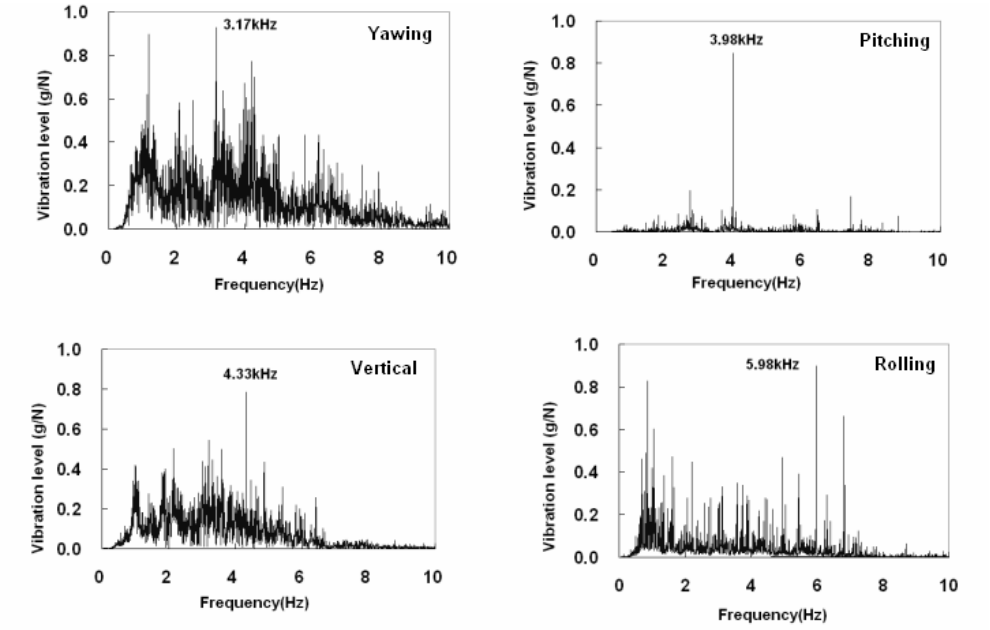

Fig. 8. Experimentally measured vibration spectra of linear guide with low preload.

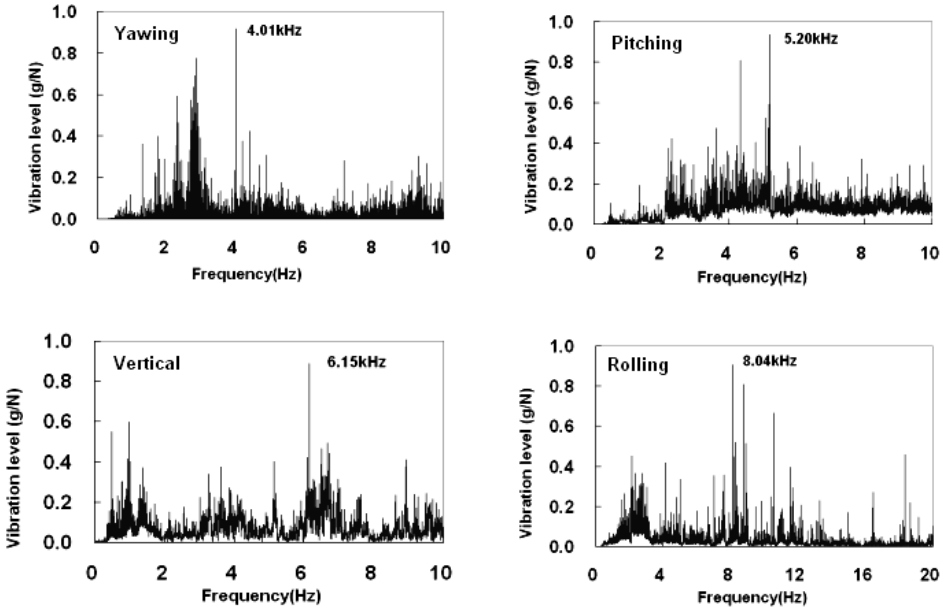

Fig. 9. Experimentally measured vibration spectra of linear guide with high preload.

each guide, which in turn is expected to cause a change in the stiffness and vibration characteristics of the stage.

4.1 Vibration test

To realize the variation of the dynamic behavior of the stage under different loading conditions, vibration tests were performed on the prototype stage in two ways: (1) the stage was, respectively, equipped with a heavily and slightly preloaded linear guide without any attachment; and (2) the stage was equipped with a lightly preloaded guide and carried an object at mid-point (x = 0) and quarter-point (x = 80 mm, a distance of 80 mm from the center of platform). Henceforth, the stages equipped with linear guides that were heavily and lightly preloaded will be referred to as high-preload and low-preload stages, respectively.

As in the vibration test of the rolling guide, the accelerometers were located at appropriate positions so that the measured vibration spectra could be used to estimate the vibration frequency corresponding to the vibration mode predicted by finite element modal analysis. Fig. 10 illustrates the loading stage assembly with two linear guides, where the accelerometers at locations A, B, C, and D were used to measure the vibration motions of the yawing, pitching, bending, and twisting modes respectively. Furthermore, an additional object with a mass of 21.1 kg was placed at different positions during the test to evaluate the loading effect.

4.2 Finite element modal analysis

To provide a comparison with the experiments, finite element modal analysis was performed to examine the vibration characteristics of the loading stage. As shown in Fig. 11, the finite element mode of the loading stage used in the vibration test was meshed with brick elements, with the mode numbering 19992 elements and 25672 nodes after the convergence test. The rolling interfaces at the ball grooves of the linear guide were simplified as surface to surface contact states and a series of spring elements were employed to connect the rail and carriage directly. It should be kept in mind that the contact force acting on the rolling ball varies according to the loading position of the objects. Accordingly, the contact stiffness at each contact point in ball groove needs to be recalculated according to the reaction of the guide to the applied load, including the preload setting on the rolling balls

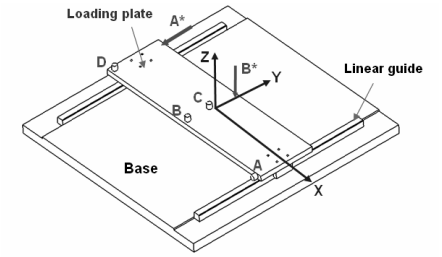

Fig. 10. Schematic of loading stage assembly with two linear guides, showing the locations of accelerometers A, B, C and D for measuring the vibration motion of yawing, pitching, bending, and twisting mode, respectively. The symbols with arrows A* and B* represent the hammering point and direction for yawing mode and pitching mode, respectively. An additional object of 21.1 Kg is placed at different positions in test.

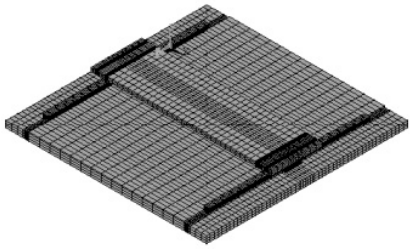

Fig. 11. Finite element model of the loading stage, including the base, loading plate and two rolling guides. The rolling interface within each linear guide was modeled by a series of spring elements, as in the case of rolling guide.

and the weight of the attached object. For further comparison between the finite element modal analysis and the experiments, the object was located at two different positions as in tests. The values of the contact stiffness of the linear guide under different loading modes are shown in Table 3.

In addition, to explore the effect of the rolling interface on the dynamic characteristics, the rolling interface of the guide was intentionally modeled with a fixed interface. Under this assumption, the rail and the carriage were assumed to be fully bonded together with no slipping or separation when the rolling guide was experiencing vibration motions.

4.3 Results and discussions

The first four vibration mode shapes of the slightly preloaded stage under no load-carrying condition and according to finite element analysis are shown in Fig.12. The first mode was a yawing vibration of the loading plate about the vertical axis (z axis), which was dominated by the yawing motion of the guide at

Table 3. Comparisons of the natural frequency of a stage, obtained from finite element prediction and vibration test (unit: Hz).

Low-preload stage (K_n = 10.325 N/μm)				High-preload stage (K_n = 19.75 N/μm)		
Vibration mode	Finite element modal analysis with different interface mode at rolling interface		Vibration test	Finite element modal analysis with different interface mode at rolling interface		Vibration test
	Fixed interface	Rolling interface		Fixed interface	Rolling interface	
Yawing	-------	111.6 (2.5%)	108.8	-------	145.6 (8.3%)	134.5
Pitching	351.2	265.4 (0.2%)	265.0	351.2	286.8 (3.3%)	277.5
Vertical	685.6	388.3 (2.1%)	380.0	685.6	470.0 (6.8%)	440.0
Rolling	895.6	793.8 (5.1%)	788.7	895.6	912.4 (8.6%)	840.0

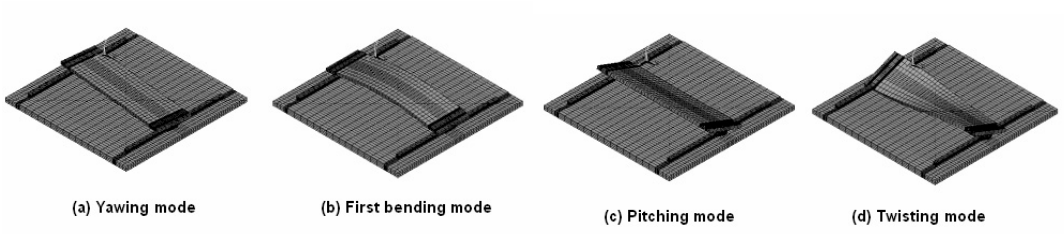

Fig. 12. Vibration mode shapes of a stage with two linear guides, (a) yawing vibration mode, (b) first bending vibration mode, (c) pitching vibration mode, (d) twisting vibration mode.

each side. The second mode was the bending vibration about the *y* axis, which was caused by the out-of-phase rolling motion of the guides. The third mode was a pitching vibration of the loading plate about the *x* axis, dominated by the in-phase pitching motions of the guides. The fourth mode was a twisting vibration of the plate about the *xy* plane, dominated by the out-of-phase pitching motion of the guides. It is obvious that the fundamental mode shapes were closely related to the vibration motions of the linear guides supporting the stage.

The vibration spectra corresponding to the measuring points A, B, C, and D are depicted in Fig. 13 for the low-preload stage and in Fig. 14 for the high-preload stage. In these figures, the main peak of each measured spectrum was identified as a natural frequency by comparing the measured vibration motion with that predicted by the finite element approach. As observed in the linear guide, the high-preload and low-preload stages demonstrated similar vibration spectra. Meanwhile, their vibration peaks were found to occur at different natural frequencies, varying with the preload of the linear guide.

Table 3 summarizes the frequencies of the unloaded stage, with those estimated by the finite element approach. The predictions of the rolling interface analysis model of the natural frequencies were in accordance with the experimentally measured results, with percentage differences of less than 8.6%; on the other hand, the natural frequencies predicted by the finite element model with a fixed interface showed greater deviations with the measured values. This implies that using the rolling interface rather than the fixed interface to model the interface among the ball grooves is more accurate in predicting the dynamic behavior of the loading stage with rolling guides. Table 3 also reveals the effect of the preload of linear guides on the vibration frequency of the stage. With a lightly preloaded guide, the stage vibrated at a lower frequency due to the lower stiffness induced at the rolling interface of the ball groove in the guide. In addition, the percentage difference between the finite element prediction and the vibration test results of the high-preload stage was found to be larger than that of the low-preload stage. This can be ascribed to the fact that (1) according to the technical manual for linear guides, the extent of preloading is in the range of 0.05-0.07 C for a heavily preloaded guide and 0.0-0.02 C for a lightly preloaded guide, where C is the dynamic load capacity. In short, the real preload of

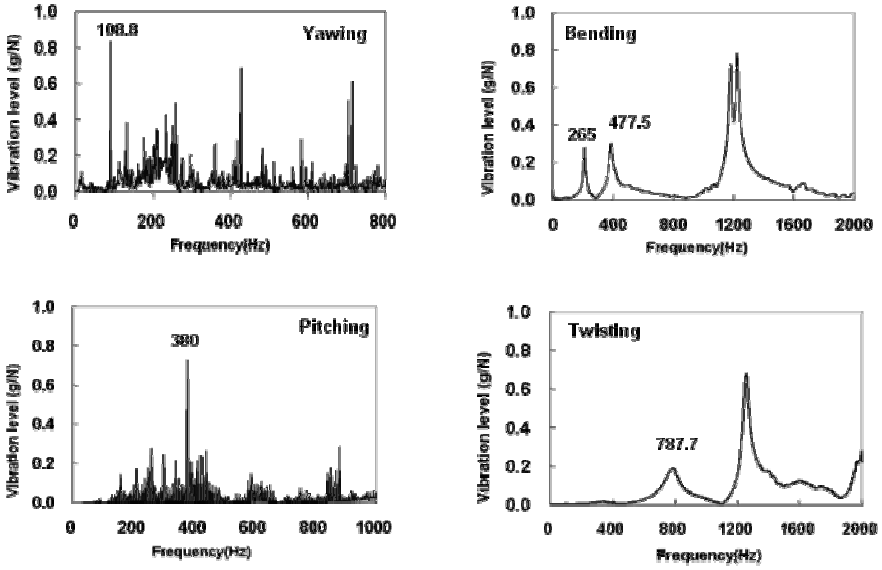

Fig. 13. Experimentally measured vibration spectra of a low-preload stage.

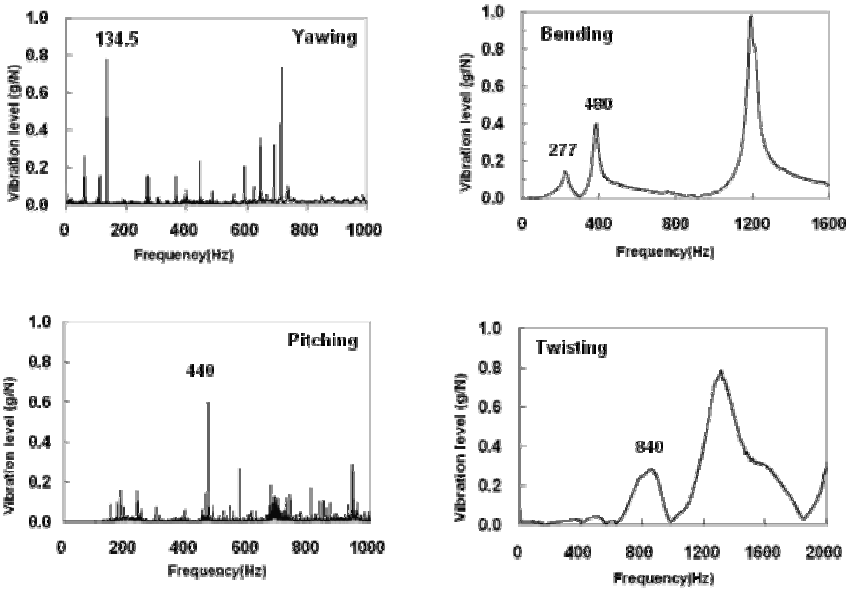

Fig. 14. Experimentally measured vibration spectra of a high-preload stage.

the linear guides used in testing could not be confirmed. (2) In the current analysis of the stage, a preload of 0.07 C was assumed in the finite element model of the high-preload stage, which may overestimate the real value of the guide employed in the vibration test and thus cause the finite element model to predict higher frequencies as compared with the vibration measurements. For low-preload stages, a mean preload of 0.01 C was assumed in the finite element mode, and the results agreed well with the vibration measurements; for the high-preload stage, if the mean value of the preload according to the technical manual (0.06 C) had been adopted for the finite element model instead of 0.07 C, the predictions of the vibration frequencies would be accordance with the measured values, with a maximum difference of 5.5%.

The results for the vibration test and the finite ele-

Table 4. Variation of natural frequency of the stage with the change of load position.(unit: Hz) (The stage is equipped with low preloaded guides in this case).

Mode shape	Case 1*			Case 2**			Case 3***		
	Unloaded stage			Stage with a mass of 21.1 Kg at mid-point, x=0			Stage with a mass of 21.1 Kg at quarter-point, x=80 mm		
	vibration test	modal analysis	percentage difference	vibration test	modal analysis	percentage difference	vibration test	modal analysis	percentage difference
Bending	265.0	265.4	0.15%	52.5	53.0	0.95%	82.5	83.78	1.55%
Yawing	108.8	111.6	2.57%	122.5	123.8	1.06%	115.0	111.71	2.86%
Pitching	380.0	388.3	2.18%	398.1	411.5	3.37%	407.5	413.27	1.42%
Twisting	788.7	793.8	0.65%	832.5	837.9	0.65%	822.5	829.87	0.90%

* The contact stiffness is $K_n = 10.325$ N/μm for all linear guides.
** The contact stiffness is $K_n = 13.28$ N/μm for all linear guides.
*** The contact stiffness of linear guides is $K_n = 12.45$ N/μm at one side and $K_n = 14.06$ N/μm at another side.

ment analysis regarding the effect of the additional load on the stage also report similar results (Table 4) for cases 1 and 2. They show that the loaded stage vibrated in the yawing, pitching, and twisting modes at higher frequencies compared to the unloaded stage. As mentioned above, these fundamental mode shapes of the stage were subtly related to the vibration motions of the linear guide. Therefore, the variations in frequency of these modes can be shown to have been induced by the increased contact stiffness of the linear guide due to excessive load acting on the balls. In contrast, the natural frequency of the loaded stage for bending vibrations was greatly decreased because the vibrating amplitude was damped by the mass attached to the loading plate.

The attached position of the additional mass was another factor affecting the vibration characteristics of the loaded stage. This can be further investigated by comparing the frequencies of the stage carrying the load at the midpoint (x = 0 mm) and quarter-point (x = 80 mm). As revealed in cases 2 and 3, when the object moved away from the midpoint the vibration frequencies corresponding to the modes for yawing and twisting decreased slightly but the modes for pitching and bending increased. There was no apparent change in the associated mode shapes. The finite element analysis predictions on the vibration characteristics have also been verified by experiments. The vibration spectra measured in the bending direction of the loading plate are shown in Fig. 15. This figure shows that the frequencies at the vibration peak shifted to different values, varying with the loading position. These results demonstrate that the mass

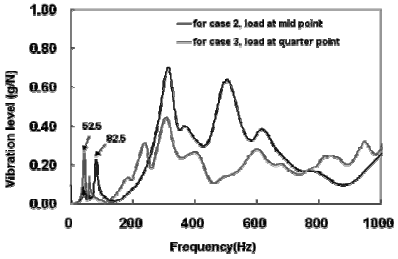

Fig. 15. Comparison of the vibration spectra in bending motion for a stage with a mass loaded at midpoint and quarter point, respectively.

effect coming from the additional mass not only caused a change in the stiffness of the guide but also enabled the stages to behave with different vibration characteristics, including the variation in mode shape and frequency.

For the three analysis cases, the percentage differences between the results obtained from the experiments and the finite element predictions were less than 3.37%. This further implies that the validity of the presented modeling method for the rolling interface was verified experimentally.

5. Conclusions

In this paper, the vibration characteristics of a preloaded rolling guide with four rows of rolling grooves were investigated to discuss the modeling of the rolling interface through finite element simulation analysis and validated with an experimental vibration test. The results of this study demonstrated that the vibration characteristic of the rolling guide was success-

fully predicted by the proposed analysis model, where spring elements were employed to simulate the rolling contact between the rolling balls and the ball grooves. The rolling balls were shown to have no apparent effect on the natural vibration frequencies of the carriage and hence were ignored in modeling the rolling interface for the finite element analysis. In the cases of loading stages with preloaded guides, the stage with a rolling interface model also predicted vibration behavior observed in experiments. In addition, the load applied to the stage was shown to have a profound influence on the vibration characteristics of the stage due to the change in contact stiffness of guide. Concluding from these results, it is suggested that such a load effect should be taken into account in investigating the dynamic characteristics of a positioning mechanism with a rolling guide.

Acknowledgments

The support from National Science Council in Taiwan (95-2622-E-167-001-CC3) is gratefully acknowledged. The author would like to thank the anonymous reviewers for their valuable suggestions.

References

[1] M. Ninomiya and S. Kato, Analysis of linear guide and ball screw stiffness, *International Journal of the Japan Society for Precision Engineering*, 33 (1999) 173-177.

[2] H. Ohta, Sound of linear guideway type recirculating linear ball bearings, *Transactions of the ASME Journal of Tribology*, 121 (1999) 678-685.

[3] H. Ohta and E. Hayashi, Vibration of linear guideway type recirculating linear ball bearings, *Journal of Sound and Vibration*, 235(5) (2000) 847-861.

[4] J. C. Chang, J. S. S. Wu and J. P. Hung, Characterization of the dynamic behavior of a linear guideway mechanism, *Structural Engineering and Mechanics*, 25(1) (2007) 1-10.

[5] J. S. S. Wu, J. C. Chang and J. P. Hung, The effect of contact characteristic on dynamic behaviors of rolling contact elements, *Mathematics and Computers in Simulation*,74(6) (2007) 454-467.

[6] T. A. Harris, An analytical method to predict skidding in thrust-loaded, angular-contact ball bearings, *ASME Journal of Lubrication Technology*, 93 (1971) 17-24.

[7] T. A. Harris, *Rolling bearing analysis*, 2nd ed, John Wiley & Sons, New York, 1984.

[8] Y. C. Shin, Bearing Nonlinearity and stability analysis in high speed machining, *ASME Journal of Engineering Industrial*, 114 (1992) 23-30.

[9] S. Kasai, T. Tsukada, and S. Kato, Recent technical trends of linear guides, *NSK Technical Journal*, 649 (1988) 27-36.

[10] J. Ye, N. Iijima, F. Tashiro, S. Hagiwara, and S. Yamada, Vibration of linear motion bearing, *Proceedings of Spring JSPE Meeting*, F14 (1988) 199-200.

[11] K. J. Johnson, *Contact mechanics*, Cambridge University Press (1985).

[12] Y. Shiroji, Development of NSK Linear Guides, *NSK Technical Journal, Motion & Control*, 5 (998) 9-18.

[13] THK CO., LTD., Features of the LM Guide, *http://www.thk.com/online_cat*.

[14] D. E. Brewe, and B. J. Hamrock, Simplified solution or elliptical-contact deformation between two elastic solid. *Journal of Lubrication Technology*, 99 (1997) 485-487.

[15] J. A. Greenwood, Analysis of elliptical Hertzian contacts, *Tribology International*, 30 (1997) 235-237.

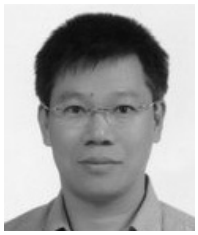

Jui-Pin Hung received the B.S. and M.S. degrees in Mechanical Engineering from National Chiao Tung University, Hsinchu, Taiwan in 1981 and 1983, respectively, and his Ph.D. degree from National Chung Hsing University in 2002. Dr. Hung is currently an associate professor at the Department of Mechanical Engineering at Chin Yi University of Technology in Taichung County, Taiwan. His research interests are in the area of machine tool design, failure analysis of mechanical components and orthopedic biomechanics.